



ORIGINAL ARTICLE

# Intelligent human computer interaction based on non redundant EMG signal



Ying Sun<sup>a,b,c</sup>, Chao Xu<sup>a</sup>, Gongfa Li<sup>a,b,c,\*</sup>, Wanfen Xu<sup>a</sup>, Jianyi Kong<sup>a,b,d</sup>,  
Du Jiang<sup>a</sup>, Bo Tao<sup>a,c,d</sup>, Disi Chen<sup>e</sup>

<sup>a</sup> Key Laboratory of Metallurgical Equipment and Control Technology of Ministry of Education, Wuhan University of Science and Technology, Wuhan 430081, China

<sup>b</sup> Institute of Precision Manufacturing, Wuhan University of Science and Technology, Wuhan 430081, China

<sup>c</sup> Research Center for Biomimetic Robot and Intelligent Measurement and Control, Wuhan University of Science and Technology, Wuhan 430081, China

<sup>d</sup> Hubei Key Laboratory of Mechanical Transmission and Manufacturing Engineering, Wuhan University of Science and Technology, Wuhan 430080, China

<sup>e</sup> School of Computing, University of Portsmouth, Portsmouth PO1 3HE, UK

Received 14 November 2019; revised 3 January 2020; accepted 8 January 2020

Available online 22 January 2020

## KEYWORDS

Human computer interaction;  
Intelligence;  
Surface electromyogram signal;  
Thumb gesture recognition;  
Redundant electrodes

**Abstract** Human computer interaction plays an increasingly important role in our life. People need more intelligent, concise and efficient human-computer interaction. It is of great significance to optimize the process of human-computer interaction by using appropriate calculation methods. In order to eliminate the interference data of thumb recognition based on sEMG signal in the process of human-computer interaction, simplify the data processing, and improve the working efficiency of general equipment of sEMG signal. In the process of gesture recognition using sEMG signals generated by thumb, a method of redundant electrode determination based on variance theory is proposed. The redundancy of five groups of action signals is divided into 16 levels and visualized. By comparing the results of thumb motion recognition when different redundant channels are removed, the optimal channel combination in the process of thumb motion recognition is obtained. Finally, two kinds of classifiers suitable for sEMG signal field are selected, and the classification results are compared, and the best method of thumb motion pattern recognition is obtained.

© 2020 The Authors. Published by Elsevier B.V. on behalf of Faculty of Engineering, Alexandria University. This is an open access article under the CC BY-NC-ND license (<http://creativecommons.org/licenses/by-nc-nd/4.0/>).

\* Corresponding author at: Key Laboratory of Metallurgical Equipment and Control Technology of Ministry of Education, Wuhan University of Science and Technology, Wuhan 430081, China.  
E-mail address: [ligongfa@wust.edu.cn](mailto:ligongfa@wust.edu.cn) (G. Li).

Peer review under responsibility of Faculty of Engineering, Alexandria University.

<https://doi.org/10.1016/j.aej.2020.01.015>

1110-0168 © 2020 The Authors. Published by Elsevier B.V. on behalf of Faculty of Engineering, Alexandria University.  
This is an open access article under the CC BY-NC-ND license (<http://creativecommons.org/licenses/by-nc-nd/4.0/>).

## 1. Introduction

Simplifying human-computer interaction process has become a research hotspot in the field of intelligent control. The diversity of gesture makes the development of human-computer interaction technology based on gesture recognition more and more important [1,2]. Surface electromyography (sEMG) signal is gradually developed in the wave of human-computer interaction. As an important means of perceiving human motion, it can not only reflect the flexion and extension function of hand joints, but also reflect the dynamic information such as the position and intensity of limbs in the process of action completion. Many scholars have done a lot of research on gesture recognition based on sEMG. The problem of electrode redundancy in thumb motion recognition by sEMG is solved by using variance theory of statistics. This method is helpful to optimize the human-computer interaction process in this field.

Surface EMG signal acquisition equipment is relatively simple, most of them are general equipment, and few of them are specially designed for specific actions of specific parts. The most direct impact of this phenomenon is that when using general equipment to collect special or fine actions, the interference signals generated by some redundant channels will not only increase the difficulty of data processing, but also affect the recognition accuracy. The innovation of this paper is to use statistical theory to eliminate redundant channels in the process of signal acquisition. It is of great significance to detect and eliminate the interference signals generated by redundant channels during the acquisition of certain specific actions by using the universal sEMG signal acquisition equipment.

Taking 16 channel sEMG acquisition equipment as the research object, common redundant electrodes can be obtained by identifying the thumb fine motion of 9 targets [3–5]. This study not only reduces the cost of hardware equipment, but also provides a reference for optimizing electrode distribution. It can also reduce the amount of data processing and save time.

The remaining arrangements are as follows. The second part introduces the related work of thumb motion recognition. See Section 3 for experimental materials and methods. The fourth part introduces the theory and calculation in the experiment. The fifth part is the experimental results and the discussion of the experimental results. See Section 6 for conclusions.

## 2. Related works

At present, the research of gesture recognition mainly focuses on the recognition and classification of large-scale gestures [6]. But in daily life, subtler hand movements, including arm, wrist and finger movements, are performed [7,8]. According to clinical research, the function of thumb is much greater than that of other fingers, and its participation is the highest in daily life. Most of the grasping movements can't be separated from the cooperation of thumb. The motion state of the thumb will affect the overall gesture, and the motion position of the thumb will also have a direct impact on the grasping effect. In the aspect of rehabilitation science, the movement of the thumb can reflect the overall posture of the hand movement to a certain extent, and the study of the thumb has a deeper understanding of the subdivision and motion characteristics of the whole hand control [9,10]. In the aspect of

human-computer interaction, a few subtle movements of the thumb can be used as commands to control the computer, which can bring more convenience to the human-computer interaction [11–14].

Gesture recognition based on surface sEMG is mainly to collect electrical signals generated on skin surface by EMG acquisition equipment, and then classify and recognize the data after feature extraction. In recent years, many scholars have studied the myoelectric signals in the field of human-computer interaction. Ying Sun et al. used the combination of image and sEMG signal to recognize gestures [15]. Xun Chen et al. studied the influence of feature and classification algorithm on recognition accuracy. In this experiment, four channels of sEMG acquisition equipment were used to collect forearm sEMG signals from ten Chinese gestures. By combining traditional features with the proposed classification algorithm, the recognition accuracy of hand motion was improved to more than 95% [16]. Jongin Kim et al. used sEMG signals to identify the scaling of the distance between index finger and thumb on the electronic screen [17]. Chengcheng Li et al. extracted four features from nine gestures and used SVM classifier to recognize gestures with a recognition rate of 98% [18]. G. F. Li etc. used tactile sensor in the process of EMG gesture recognition [19]. Nor Anija Jalaludin et al. designed a device to detect the strength of sEMG and thumb, and established the sEMG model of the relationship between the angle and force of thumb [20]. This paper optimizes the method of thumb motion recognition based on sEMG signal. Essam odah et al optimize hand tools by testing the pressure of different holding positions with sEMG signals [21].

The use of sEMG signals to identify hand movements requires analysis of the muscles of the hand. This study needs to optimize the process of thumb movement recognition, so the analysis of thumb muscles is essential [22].

The muscle groups connected to the thumb can be divided into internal and external muscle groups [23,24]. The inner adnexal muscle group was mainly distributed in the hand, and the outer adnexal muscle group was mainly distributed on the arm. The inside muscle group is composed of abductor pollicis transversus, flexor pollicis brevis, first dorsal interosus, opponens pollicis and abductor pollicis brevis. The outside muscle group is composed of flexor pollicis longus, extensor pollicis brevis and abductor pollicis longus (see Fig. 1 and Table 1).

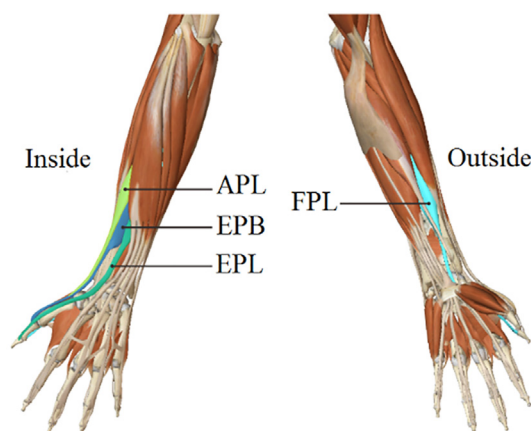


Fig. 1 The outside muscle group.

Muscle type	Name	Abbreviation
Inside muscle group	Abductor Pollicis Transverus	AP
	Flexor Pollicis Brevis	FPB
	First Dorsal Interossum	FDI
	Opponent pollicis	OP
	Abductor Pollicis Brevis	APB
Outside muscle group	Flexor Pollicis Longus	FPL
	Extensor Pollicis Longus	EPL
	Extensor Pollicis Brevis	EPB
	Abductor Pollicis Longus	APL

### 3. Material and methods

#### 3.1. Selection of acquisition equipment

The main function of the sEMG acquisition equipment is to store and filter the electrical signals generated by the skin surface. Because the sEMG signal is a weak and easy to interfere with the bioelectric signal, so the quality of the signal is closely related to the equipment [25,26]. The equipment selected in this paper adopts 16-channel high spatio-temporal resolution sampling technology, which is compatible with a variety of dry and wet electrodes and Bluetooth wireless communication technology, and can be used for gait analysis, muscle fatigue analysis, rehabilitation treatment, gesture recognition and so on. This equipment is also the commonest equipment on the market to collect the upper limb sEMG signals. It can basically meet most research tasks based on EMG signals. The experimental equipment is shown in Fig. 2. The sEMG signal acquisition system used in this paper is customized by the intelligent system and biomedical robot group of the University of Portsmouth UK. The electrode sleeve is designed with 18 dry electrodes embedded in the flexible fabric to form 16 bipolar sEMG channels, and an empty sleeve is attached to reduce the use of artifacts. Among the 18 electrodes, one is the grounding electrode, the other is the reference electrode, and the other 16 electrodes are evenly distributed inside the sleeve. The main equipment of sEMG acquisition is a host using high spatial-temporal resolution sampling technology, which can be compatible with various types of dry and wet electrodes



Fig. 2 Experimental equipment.

through Bluetooth wireless communication transmission [27–29]. After the sEMG host and the computer host are paired by Bluetooth, they can enter the sEMG signal acquisition interface. The software matching the hardware is myoanalytics 2.0. It can do some proper debugging in the signal acquisition preprocessing, such as setting up small and large window, translation distance, signal acquisition time, extracting several basic features according to the signal characteristics. In the same time, two modes of on-line and off-line analysis can be provided according to the research needs [30,31]. Because the article needs to do other analysis on the original signal, it adopts off-line analysis.

#### 3.2. Experimental process design

Since an international standard for judging flexibility has been designed for fingers, the core of the standard is whether the thumb can easily touch the other four fingers, so we selected five dynamic gestures according to the standard [32,33].

They are thumb upward movement-relax (UP), thumb downward movement-relax (DOWM), thumb left movement-relax (LEFT), thumb right movement-relax (RIGHT), thumb press-relax (PRESS). The actual actions of the five gestures are shown in Fig. 3.

A total of 9 subjects, including 2 women and 7 men, aged between 25 and 30 years old, were healthy and had no history of motor nerve, and there was no high intensity activity in the week before the experiment.

The experiment requires that in the process of data acquisition, the subjects should keep their sitting position, put their elbows on the table, and their forearms should be suspended naturally. Each subject needs to measure five sets of data, each of which includes five types of gestures, each of which is repeated ten times. A gesture cycle is 10 s, the first 5 s are the receipt collection phase, the last 5 s are the relaxation phase [34,35]. The gesture data of 9 subjects were collected for 5 days. There were 2250 gestures in the whole data set.

### 4. Theory and calculation

#### 4.1. Wave filtering

Wave filtering is an operation to filter out the frequency of specific band in the signal, and it is an important measure to

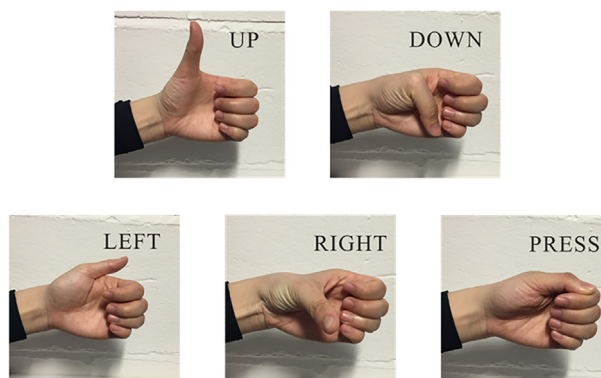


Fig. 3 Five gestures.

suppress and prevent interference. The digital filter converts the discrete input signal into another discrete output signal according to the actual need, as shown in block Fig. 4 [36].

Because the sEMG signal is very weak, it is necessary to amplify the electric signal collected by the front electrode through the pre amplification circuit. In the second step, the high pass filter and the low pass filter are used to filter the wake noise within 20 Hz and the ambient noise above 500 Hz. Then through the comb filter of 50 Hz, the power frequency noise caused by the power frequency induction phenomenon inside the acquisition device is removed as much as possible. Finally, the filtered signal is amplified twice to fit the acquisition equipment.

#### 4.2. Active segment detection

In the experiment, the five gestures are all dynamic, and the five seconds of relaxing time when collecting data is not accurate enough. So we must get rid of the redundant signals of the relaxation time, and the intercepted gesture signals must also include the whole movement process, and the task of the activity segment detection is to determine the start and end of the gesture [37–39]. The moving average method uses a certain window width to slide on the signal, and compares the instantaneous energy sequence of the signal with the preset threshold value in real time, so as to determine the start and end point of the gesture signal [40]. The signal value of sEMG changes from positive to negative in a short period of time, and the random fluctuation is relatively large, the moving average method is conducive to eliminate the interference fluctuation and get the overall trend of the signal. The overall process is as follows.

- (1) By summing and averaging the channel signals, an average sEMG sequence  $\bar{s}(t)$  reflecting the execution and relaxation periods of gestures can be obtained. The formula is shown in Eq. (1):

$$\bar{s}(t) = \frac{1}{C} \sum_{c=1}^C s_c(t) \quad (1)$$

where  $C$  is the number of sEMG channels and  $c$  is the channel label, and  $1 \leq c \leq C$ .  $S_c(t)$  is the instantaneous EMG sequence.

- (2) Using active window width  $W = 300$ , the instantaneous energy sequence of signal is averaged by moving item by item, and the moving average sequence  $E_{MA}(t)$  is obtained, as shown in Eq. (2).  $E(i)$   $t$  is the instantaneous energy sequence.

$$E_{MA}(t) = \frac{1}{W} \sum_{i=t-W+1}^t E(i) \quad t \geq W \quad (2)$$

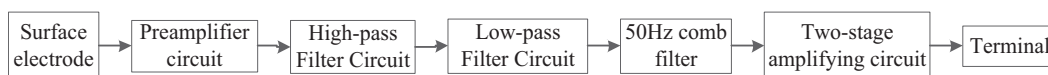


Fig. 4 Signal processing flow.

- (3) Choose appropriate threshold and process the signal sequence after moving average to determine the starting point and ending point of the active segment: the starting point is defined as the point where the moving average signal just exceeds the threshold, and the ending point is defined as the point where the average signal just falls below the threshold [41]. The selection of threshold is determined by the effect of the experiment. The larger the noise of the collected signal is, the larger the setting of threshold is. The signal quality of this paper is better, so the selected threshold is 3% of the instantaneous energy peak.

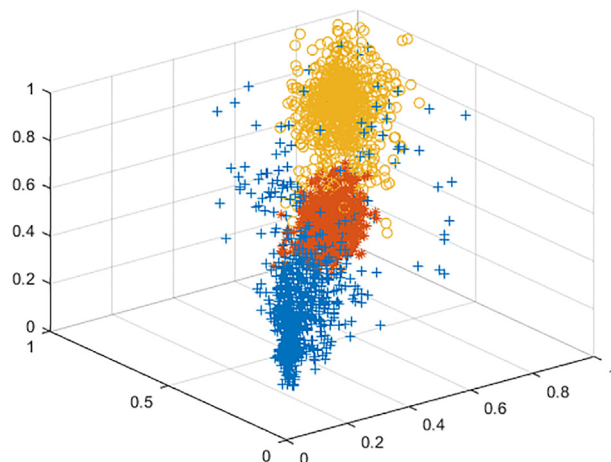


Fig. 5 Effect of feature clustering.

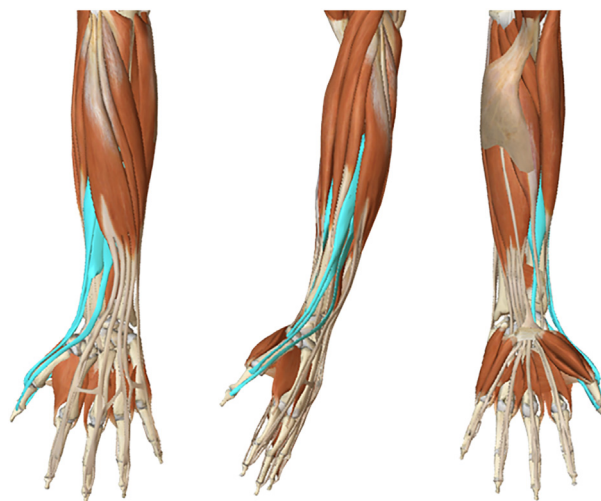


Fig. 6 Surface EMG signal generation region.

- (4) According to the starting point and the end point, the active segment whose data point length is less than a certain value is removed as noise.

$$\text{Feature} = \{SSC, RMS, AR\} \tag{3}$$

4.3. Feature extraction

The best ones are selected from six common time-domain methods, which are mean absolute value feature, slope sign change feature, zero-crossing feature, waveform length feature, autoregressive model and root mean square [42–44]. Through clustering validation, it is found that the combination of SSC, RMS and AR has the best classification effect [45–47]. The effect of feature clustering is shown in Fig. 5.

4.4. Redundant electrode selection

The sEMG acquisition equipment used is composed of 16 electrodes evenly distributed in the forearm. However, in the process of collecting sEMG signals of different parts, not all motor signals are useful. The external muscle groups that produce signals mainly concentrate in the blue area of the Fig. 6. In theory, there is no sEMG signal related to thumb outside the blue area. In the actual operation process, factors such as muscle linkage and electrode displacement increase the area of signals generated in the forearm, but for uniformity. Redundant sEMG still exists in 16-channel distributed devices [48].

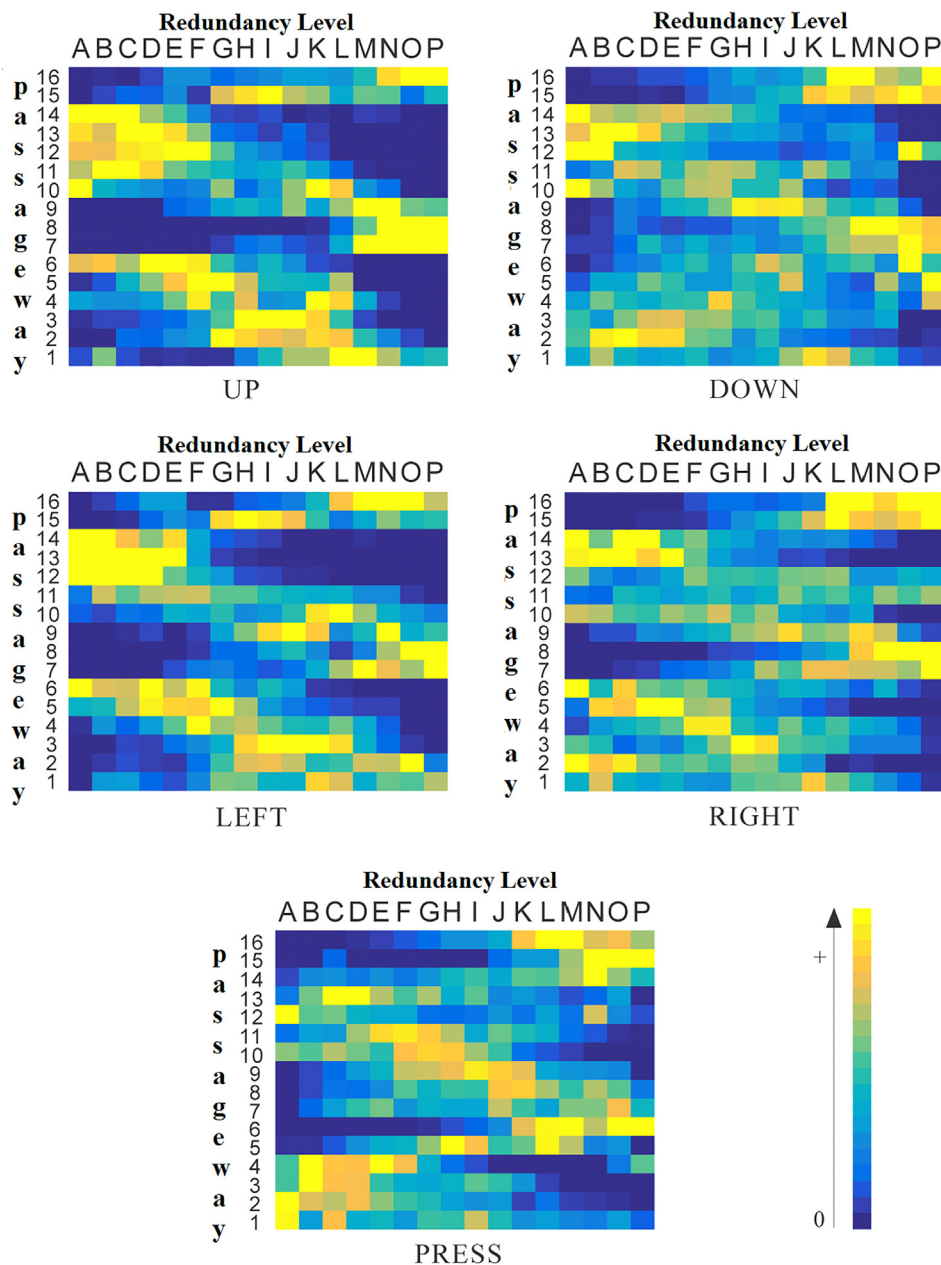


Fig. 7 Channel redundancy visualization.

Variance is a measure of the degree of deviation of data, which can represent the degree of redundancy of sEMG time domain information.

When we make the five thumb gestures as shown in Fig. 2 above, the collected sEMG signals will change, and the change degree of the signals from the 16 channels is also different. Based on the signal value when we don't do the actions, the sEMG signals of the 16 channels are variance calculated.

The larger the variance value is, the more active the signal is, and the smaller the variance value is, the more redundant the signal is.

$$VAR = \frac{1}{N-1} \sum_{i=1}^N x_i^2 \tag{4}$$

The redundancy of each channel signal is divided into 16 levels, and the redundancy is gradually reduced from A to P. Fig. 7 can be obtained by grading and visualizing the redundancy of each channel in each action using the above variance calculation value [49,50].

The depth of the color in the image represents the number of redundancy occurrences. The dark region indicates that the number of redundancy occurrences is less in this channel, while the light region indicates that the number of redundancy occurrences is more in this channel. Because the redundancy level is proportional to the weight, the weight of redundancy A to redundancy P decreases step by step. We use simple sequencing coding method to assign weight to each level [51–54]. The corresponding relationship between weight and coding is shown in Eq. (5).

$$W_i = \frac{C_i}{\sum_{i=A}^P C_i} \tag{5}$$

where i denotes grade A to grade P; C denotes natural number coefficient; W denotes weight. The specific relationship is shown in Table 2.

At the same time, in order to ensure the robustness of the data, the cross validation method [55,56] is used here to separate the data of one group of subjects, and the data of the other eight groups of subjects are combined into a sub database for testing. After nine repetitions in turn, the weighted redundancy rate of 16 channels is shown in Fig. 8.

According to the weighted results, there are three kinds of public redundant channels, which are:

- (1) 13
- (2) 12, 13, 14
- (3) 2, 3, 4, 5, 6, 10, 11, 12, 13, 14

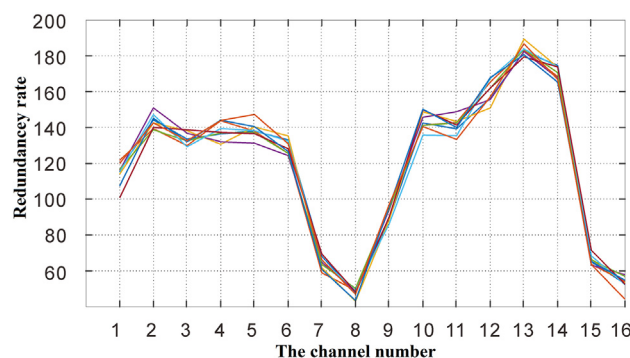


Fig. 8 Weighted Channel Redundancy.

### 5. Results and discussion

In order to get better results, we must select a classifier with certain feature advantages. At present, the mainstream limb motion pattern classifiers include: artificial neural network (ANN), linear discriminant analysis (LDA), support vector machine (SVM), Gaussian mixture model (GMM), hidden Markov model (HMM), generalized regression neural network (GRNN), etc. Among them, SVM has excellent performance, its meticulous mathematical theory and good classification performance make it widely used in the field of electromyography, so SVM is the first choice classifier for experiments; GRNN has strong approximation ability and strong approximation ability and classification ability, and its learning speed is better than BP (error back propagation algorithm) neural network and RBF (radial phase basis) neural network, and it is good at To deal with the problem of data classification under noise, GRNN is used as the second choice classifier.

There are 2250 data samples in this experiment. 90% of them are used as training data, 10% as test, cross validation 10 groups, each group has 225 test samples. The SVM algorithm is selected as the reference classifier, and the above three results are classified respectively. The results are as follows.

From the Fig. 9, we can see that after removing 10 redundant channels, the recognition accuracy is significantly reduced, but when removing channels 13 and 12, 13 and 14, the accuracy is almost unchanged. Under the premise of keeping the recognition accuracy unchanged, more redundant channels are selected to be removed, including channels 12, 13 and 14. After removing three channels, the training time of classifier is reduced by nearly 20%.

The generalized regression neural network (GRNN) is a deformation of traditional radial basis function (RBF) network based on mathematical statistics, which is mainly used for regression analysis of nonlinear data [57–59]. Its nonlinear mapping ability and training speed are better than RBF

Table 2 Redundancy levels and weights.

Redundancy level	Most redundant Most active															
	A	B	C	D	E	F	G	H	I	J	K	L	M	N	O	P
Coefficient	16	15	14	13	12	11	10	9	8	7	6	5	4	3	2	1
Weight	0.117	0.110	0.103	0.096	0.088	0.080	0.074	0.066	0.058	0.051	0.044	0.036	0.029	0.022	0.015	0.007

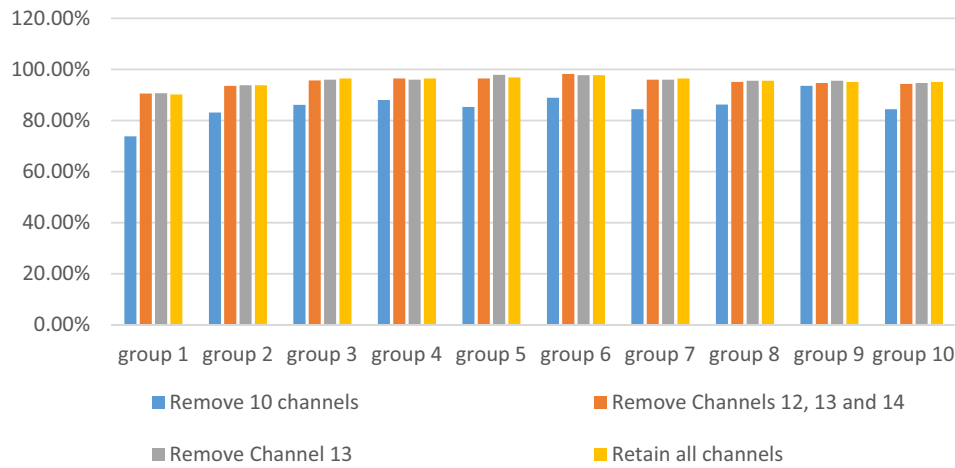


Fig. 9 Remove redundant channels and retaining the average classification accuracy of all channels.

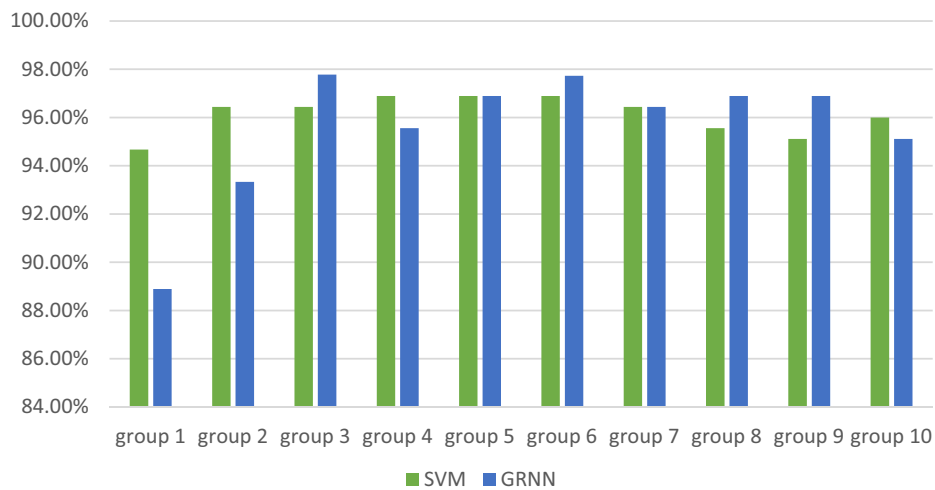


Fig. 10 Classification results of 16 channels reserved by SVM and GRNN.

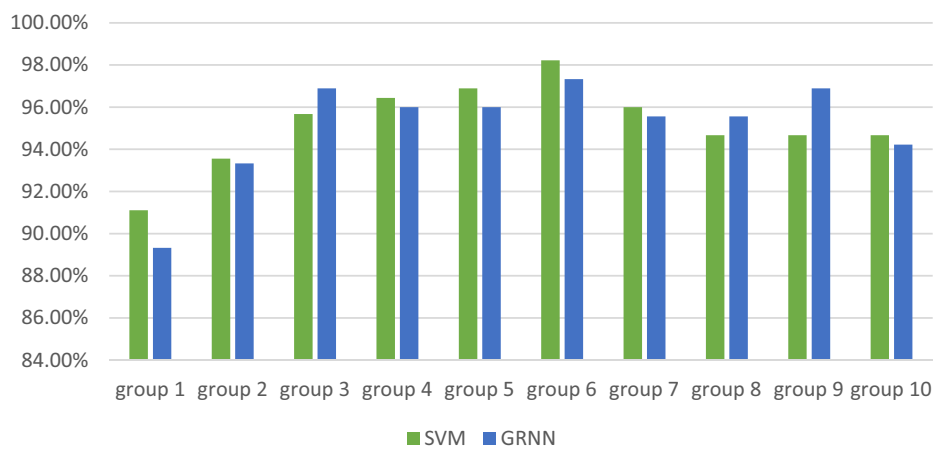


Fig. 11 Classification results of channels 12, 13 and 14 removed by SVM and GRNN.

network, and its nonlinear fitting ability, classification ability and training speed are better than BP neural network. GRNN is similar to RBF in structure, and generally consists of four layers: input layer, mode layer, summation layer and output

layer. The number of neurons in the input layer of GRNN network is the same as the dimension of the input vector in the training set samples, and each neuron directly transfers it to the model layer after receiving the data [60]. In the experiment,

the number of neurons in the input layer is 52; the number of neurons in the model layer is equal to the total number of learning samples, and each neuron distribution corresponds to different samples; the number of neurons in the sum layer is related to the total number of samples, In this paper, the number of neurons in this layer is 5; the number of neurons in the output layer is generally equal to the total number of samples.

By comparing Figs. 10 and 11, it can be seen that the recognition rate of SVM is slightly better than GRNN, and the robustness is obviously better than GRNN, whether all channels are reserved or 12, 13 and 14 channels are removed. Therefore, the redundant channel removed in this paper is not only suitable for SVM, but also for other classifiers.

## 6. Conclusion

First, the dynamic gestures are determined, the raw data is collected, the raw data is filtered, active segment detection, and feature selection are performed. Then, the redundancy of each channel electrode was calculated by using the variance theory. Three types of redundant electrode combinations were obtained by using a simple coding method. SVM was selected as the reference classifier, and the 12, 13, 14 channels were removed as the best. Finally, by comparing the classification effect of SVM and GRNN in 16-channel and 13-channel, it is proved that the removed redundant electrodes are common redundant electrodes.

## Declaration of Competing Interest

The authors declare that there is no conflict of interest regarding the publication of this article.

## Acknowledgements

This work was supported by grants of Hubei Provincial Department of Education (D20191105).

## References

- [1] G.F. Li, H. Wu, G.Z. Jiang, S. Xu, H.H. Liu, Dynamic gesture recognition in the internet of things, *IEEE Access* 7 (2019) 23713–23724.
- [2] M. Balouchestani, S. Krishnan, Robust compressive sensing algorithm for wireless surface electromyography applications, *Biomed. Sign. Process. Control* 20 (2015) 100–106.
- [3] Z. Jiang, Y. Jiang, Y. Wang, H. Zhang, H.J.C.G.D. Tian, A hybrid approach of rough set and case-based reasoning to remanufacturing process planning, *J. Intell. Manuf.* 30 (1) (2019) 19–32.
- [4] G.R. Naik, S.E. Suvisheshamuthu, M. Gobbo, Principal component analysis applied to surface electromyography: a comprehensive review, *IEEE Access* 4 (2016) 4025–4037.
- [5] H. Wang, Z.G. Jiang, H. Zhang, Y. Wang, Y.H. Yang, Y. Li, An integrated MCDM approach considering demands-matching for reverse logistics, *J. Clean. Prod.* 208 (2019) 199–210.
- [6] D.S. Chen, G.F. Li, Y. Sun, J.Y. Kong, G.Z. Jiang, H. Tang, Z. J. Ju, H. Yu, H.H. Liu, An interactive image segmentation method in hand gesture recognition, *Sensors* 17 (2) (2017) 253.
- [7] S. Mustafa, I. Elghandour, M.A. Ismail, A machine learning approach for predicting execution time of spark jobs, *Alexandr. Eng. J.* 57 (1) (2018) 3767–3778.
- [8] M. Tavakoli, C. Benussi, J.L. Lourenco, Single channel surface EMG control of advanced prosthetic hands: a simple, low cost and efficient approach, *Exp. Syst. Applic.* 79 (2017) 322–332.
- [9] J.B. Hu, Y. Sun, G.F. Li, G.Z. Jiang, B. Tao, Probability analysis for grasp planning facing the field of medical robotics, *Measurement* 141 (2019) 227–234.
- [10] G.F. Li, D. Jiang, Y.L. Zhou, G.Z. Jiang, J.Y. Kong, Gunasekaran Manogaran, Human lesion detection method based on image information and brain signal, *IEEE Access* 7 (2019) 11533–11542.
- [11] A.R. Siddiqi, S.N. Sidek, A. Khorshidtalab, Signal Processing of EMG Signal for Continuous Thumb-Angle Estimation, *IECON*, 2015, pp. 374–379.
- [12] J.X. Qi, G.Z. Jiang, G.F. Li, Y. Sun, B. Tao, Intelligent human-computer interaction based on surface EMG gesture recognition, *IEEE Access* 7 (2019) 61378–61387.
- [13] Y.F. Fang, D.L. Zhou, K.R. Li, H.H. Liu, Interface prostheses with classifier-feedback-based user training, *IEEE Trans. Biomed. Eng.* 64 (11) (2017) 2575–2583.
- [14] R. Menon, C.G. Di, H. Lakany, L. Petropoulakis, B. Conway, J. Soraghan, Study on interaction between temporal and spatial information in classification of EMG signals in myoelectric prostheses 1–1, *IEEE Trans. Neural Syst. Rehabil. Eng.* (2017), <https://doi.org/10.1109/TNSRE.2017.2687761>.
- [15] Y. Sun, C.Q. Li, G.F. Li, G.Z. Jiang, D. Jiang, H.H. Liu, Z.G. Zheng, W.N. Shu, Gesture recognition based on kinect and sEMG signal fusion, *Mobile Netw. Applic.* 23 (4) (2018) 797–805.
- [16] X. Chen, Z.J. Wang, Pattern recognition of number gestures based on a wireless surface EMG system, *Biomed. Signal Process. Control* (2013) 184–192.
- [17] J. Kim, D. Cho, K. Lee, B. Lee, A real-time pinch-to-zoom motion detection by means of a surface EMG-based human-computer interface, *Sensors* 15 (1) (2014) 394–407.
- [18] C.C. Li, G.F. Li, G.Z. Jiang, D.S. Chen, H.H. Liu, Surface EMG data aggregation processing for intelligent prosthetic action recognition, *Neural Comput. Appl.* (2018), <https://doi.org/10.1007/s00521-018-3909-z>.
- [19] G.F. Li, L.L. Zhang, Y. Sun, J.Y. Kong, Towards the sEMG hand: internet of things sensors and haptic feedback application, *Multim. Tools Applic.* 78 (21) (2019) 29765–29782.
- [20] N.A. Aranceta, B.A. Conway, Differentiating variations in thumb position from recordings of the surface electromyogram in adults performing static grips, a proof of concept study, *Front. Bioeng. Biotechnol.* 7 (2019), <https://doi.org/10.3389/fbioe.2019.00123>.
- [21] E. Odah, I. Abu-Qasmieh, N. Al Khateeb, E. Al Matalbeh, S. Quraan, M. Mohammad, Gender considerations in optimizing usability design of hand-tool by testing hand stress using SEMG signal analysis, *Alexandr. Eng. J.* 57 (4) (2018) 2897–2901.
- [22] K. Usha, M. Ezhilarasan, Fusion of geometric and texture features for finger knuckle surface recognition, *AEJ – Alexandr. Eng. J.* 55 (1) (2016) 683–697.
- [23] S. Kim, J. Kim, M. Kim, S. Kim, J. Park, Grasping force estimation by sEMG signals and arm posture: tensor decomposition approach, *J. Bion. Eng.* 16 (3) (2019) 455–467.
- [24] R.R. Muhammad, N.S. Shahrul, F.T. Siti, Portable thumb training system for EMG signal measurement and analysis, in: *International Conference on Computer and Communication Engineering*, 2016, <https://doi.org/10.1109/ICCCE.2016.44>.
- [25] D. Jiang, G.F. Li, Y. Sun, J.Y. Kong, B. Tao, D. Chen, Grip strength forecast and rehabilitative guidance based on adaptive neural fuzzy inference system using sEMG, *Pers. Ubiquit. Comput.* (2019), <https://doi.org/10.1007/s00779-019-01268-3>.
- [26] Z.O. Khokhar, Pattern Recognition of Surface Electromyography Signals for Real-time Control of Wrist Exoskeletons, vol. 9, 2010, pp. 24–41.

- [27] D. Jiang, Z.J. Zheng, G.F. Li, Y. Sun, J.Y. Kong, G.Z. Jiang, H. G. Xiong, B. Tao, S. Xu, H.H. Liu, Z.J. Ju, Gesture recognition based on binocular vision, *Clust. Comput.* 22 (Supplement 6) (2019) 13261–13271.
- [28] M.C. Yu, G.F. Li, D. Jiang, G.Z. Jiang, F. Zeng, H.Y. Zhao, D. S. Chen, Application of Pso-Rbf neural network in gesture recognition of continuous surface EMG signals, *J. Intell. Fuzzy Syst.* (2019), <https://doi.org/10.3233/jifs-179535>.
- [29] Y.W. Cheng, G.F. Li, J.H. Li, Y. Sun, G.Z. Jiang, F. Zeng, H. Y. Zhao, D.S. Chen, Visualization of activated muscle area based on sEMG, *J. Intell. Fuzzy Syst.* (2019), <https://doi.org/10.3233/jifs-179549>.
- [30] Y. He, G.F. Li, Y.J. Liao, Y. Sun, J.Y. Kong, G.Z. Jiang, D. Jiang, H.H. Liu, Gesture recognition based on an improved local sparse representation classification algorithm, *Clust. Comput.* 22 (Supplement 5) (2019) 10935–10946.
- [31] E.N. Kamavuako, D. Farina, K. Yoshida, W. Jensen, Estimation of grasping force from features of intramuscular EMG signals with mirrored bilateral training, *Ann. Biomed. Eng.* 40 (3) (2012) 648–656.
- [32] X. Zhai, B. Jelfs, R.H. Chan, Short latency hand movement classification based on surface EMG spectrogram with PCA, in: *Conf Proc IEEE Eng Med Biol Soc*, 2016, pp. 327–330.
- [33] M. Kim, K. Kim, W.K. Chung, Simple and fast compensation of sEMG interface rotation for robust hand motion recognition I–I, *IEEE Trans. Neural Syst. Rehabil. Eng.* (2018).
- [34] Kasiprasad Mannepalli, Panyam Narahari Sastry, Maloji Suman, A novel adaptive fractional deep belief networks for speaker emotion recognition, *Alexandr. Eng. J.* 56 (4) (2017) 485–497. <https://linkinghub.elsevier.com/retrieve/pii/S1110016816302484>, <https://doi.org/10.1016/j.aej.2016.09.002>.
- [35] H. Kalani, S. Moghimi, A. Akbarzadeh, SEMG-based prediction of masticatory kinematics in rhythmic clenching movements, *Biomed. Sign. Process. Control* 20 (2015) 24–34.
- [36] T. Al, A. Ahmad, J. Al, Adel, Optimal Feature Set for Finger Movement Classification Based on SEMG, *IEEE Engineering in Medicine and Biology Society*, 2018, pp. 5228–5231.
- [37] M.C. Yu, G.F. Li, D. Jiang, G.Z. Jiang, B. Tao, D.S. Chen, Hand medical monitoring system based on machine learning and optimal EMG feature set, *Pers. Ubiquit. Comput.* (2019), <https://doi.org/10.1007/s00779-019-01285-2>.
- [38] M.R. Al-Mulla, F. Sepulveda, Super wavelet for sEMG signal extraction during dynamic fatiguing contractions, *J. Med. Syst.* 39 (1) (2015) 167.
- [39] T.F. Yang, J.W. Wang, Z.G. Hu, Variation of neck electromyography and mechanical characteristics during the process of cervical traction, *J. Med. Biomech.* 31 (5) (2016) 421–425.
- [40] K. Veer, T. Sharma, A novel feature extraction for robust EMG pattern recognition, *J. Med. Eng. Technol.* 40 (4) (2016) 6.
- [41] S. Guo, M. Pang, B. Gao, Comparison of sEMG-based feature extraction and motion classification methods for upper-limb movement, *Sensors* 15 (4) (2015) 9022–9038.
- [42] J.X. Qi, G.Z. Jiang, G.F. Li, Y. Sun, B. Tao, Surface EMG hand gesture recognition system based on PCA and GRNN, *Neural Comput. Appl.* (2019), <https://doi.org/10.1007/s00521-019-04142-8>.
- [43] O.A. Moura Karina, R.S. Ruschel, A. Balbinot, Fault-Tolerant Sensor Detection of sEMG Signals: Quality Analysis Using a Two-Class Support Vector Machine, *IEEE Engineering in Medicine and Biology Society*, 2018, pp. 5644–5647.
- [44] P. Karthick, G. Venugopal, S. Ramakrishnan, Analysis of Muscle Fatigue Progression using Cyclostationary Property of Surface Electromyography Signals, *Plenum Press*, 2016, <https://doi.org/10.1007/s10916-015-0394-0>.
- [45] G.F. Li, J.H. Li, Z.J. Ju, Y. Sun, J.Y. Kong, A novel feature extraction method for machine learning based on surface electromyography from healthy brain, *Neural Comput. Appl.* 31 (12) (2019) 9013–9022.
- [46] G.F. Li, H. Tang, Y. Sun, J.Y. Kong, G.Z. Jiang, D. Jiang, B. Tao, S. Xu, H.H. Liu, Hand gesture recognition based on convolution neural network, *Clust. Comput.* 22 (Supplement 2) (2019) 2719–2729.
- [47] M. Nisser, S. Derlien, U.C. Smolenski, N. Best, Measurement of muscular load with sEMG in using different computer input devices - a pilot study, *Physikalische Medizin Rehabilitationsmedizin Kurortmedizin* 28 (2018) 231–234.
- [48] D. Kaneishi, R.P. Matthew, M. Tomizuka, A sEMG Classification Framework with Less Training Data, *IEEE Engineering in Medicine and Biology Society*, 2018, pp. 1680–1684.
- [49] B. Zhou, X.L. Ji, R. Zhang, Design of surface EMG acquisition instrument based on embedded technology, *Mod. Electr. Tech.* 33 (6) (2010) 55–57.
- [50] B.W. Luo, Y. Sun, G.F. Li, D.S. Chen, Z.J. Ju, Decomposition algorithm for depth image of human health posture based on brain health, *Neural Comput. Appl.* (2019), <https://doi.org/10.1007/s00521-019-04141-9>.
- [51] C. Tan, Y. Sun, G.F. Li, G.Z. Jiang, D.S. Chen, H.H. Liu, Research on gesture recognition of smart data fusion features in the IoT, *Neural Comput. Appl.* (2019), <https://doi.org/10.1007/s00521-019-04023-0>.
- [52] C. Fu, Q. Li, B. Li, Detection and noise reduction of surface electromyography signal, *Prog. Mod. Biomed.* 11 (20) (2011) 3951–3953.
- [53] T.A. Kuiken, L.A. Miller, R.D. Lipschutz, et al, Targeted reinnervation for enhanced prosthetic arm function in a woman with a proximal amputation: a case study, *Lancet (North American Edition)* 369 (9559) (2007) 371–380.
- [54] P.M.M. Balata, H.J.D. Silva Pernambuco, Leandro de Araújo, et al, Normalization patterns of the surface electromyographic signal in the phonation evaluation, *J. Voice* 29 (1) (2015) 129.e1–129.e8.
- [55] W.T. Cheng, Y. Sun, G.F. Li, G.Z. Jiang, H.H. Liu, Jointly network: a network based on CNN and RBM for gesture recognition, *Neural Comput. Appl.* 31 (Supplement 1) (2019) 309–323.
- [56] Y.J. Liao, Y. Sun, G.F. Li, J.Y. Kong, G.Z. Jiang, D. Jiang, H. B. Cai, Z.J. Ju, H. Yu, H.H. Liu, Simultaneous calibration: a joint optimization approach for multiple kinect and external cameras, *Sensors* 17 (7) (2017) 1491.
- [57] R. Crepin, C.L. Fall, Q. Mascret, C. Gosselin, L.A. Campeau, B. Gosselin, Real-time hand motion recognition using sEMG patterns classification, *IEEE Engineering in Medicine and Biology Society*, 2018, pp. 2655–2658, <https://doi.org/10.1109/EMBC.2018.8512820>.
- [58] D. Jiang, G.F. Li, Y. Sun, J.Y. Kong, B. Tao, Gesture recognition based on skeletonization algorithm and CNN with ASL database, *Multim. Tools Applic.* 78 (21) (2019) 29953–29970.
- [59] P.A. Kaplanis, C.S. Pattichis, L.J. Hadjileontiadis, V.C. Roberts, Surface EMG analysis on normal subjects based on isometric voluntary contraction, *J. Electromyogr. Kinesiol.* 19 (1) (2009) 157–171. <https://linkinghub.elsevier.com/retrieve/pii/S1505641107000636>, <https://doi.org/10.1016/j.jelekin.2007.03.010>.
- [60] B. Li, Y. Sun, G.F. Li, J.Y. Kong, G.Z. Jiang, D. Jiang, H.H. Liu, Gesture recognition based on modified adaptive orthogonal matching pursuit algorithm, *Clust. Comput.* 22 (Supplement 1) (2019) 503–512.